Lipopolysaccharide-induced Activation of NFκB Non-Canonical Pathway Requires BCL10 Serine 138 and NIK Phosphorylations

Sumit Bhattacharyya

Alip Borthakur

Pradeep K. Dudeja

Joanne K. Tobacman

Department of Medicine, University of Illinois at Chicago and

Jesse Brown VA Medical Center, Chicago, Illinois, 60612-7227

Running Title: BCL10 and NIK Required for LPS Effect on NFκB

Current support: Department of Veterans Affairs and the NIDDK (R01-DK54016, R01-DK81858 and PO1-DK67887.

Address correspondence to:
Joanne K. Tobacman
840 S. Damen Ave.
CSN 440 M/C 718
Chicago, IL 60612-7227
E-mail: jkt@uic.edu
Telephone: 312-569-7826
Fax: 312-413-8283

Abbreviations:
BCL10 - B-cell lymphoma/leukemia 10
IKK - IkappaB kinase
IκBα - Inhibitor of kappaB alpha
LPS - Lipopolysaccharide
MEF - Mouse Embryonic Fibroblast
NF-κB - Nuclear Factor kappa B
NIK - nuclear factor kappaB inducing kinase

Contributions:
S.B. - study concept and design; acquisition and analysis and interpretation of data; drafting of the manuscript; statistical analysis
A.B. - study concept and design; created BCL10 constructs
P.K.D. - study concept and design; material support
J.K.T. – study concept and design; analysis and interpretation of data; drafting of the manuscript; obtained funding

Abstract

Background and Aims: B-cell lymphoma / leukemia (BCL)-10 and reactive oxygen species mediate two pathways of NF-κB (RelA) activation by lipopolysaccharide (LPS) in human colonic epithelial cells. The pathway for LPS activation of RelB by the non-canonical pathway (RelB) in non-myeloid cells was not yet reported, but important for understanding the range of potential microbial LPS-induced effects in inflammatory bowel disease.

Methods: Experiments were performed in human colonic epithelial cells and in mouse embryonic fibroblasts deficient in components of the IkappaB kinase (IKK) signalosome, in order to detect mediators of the non-canonical pathway of NFκB activation, including nuclear RelB and p52 and phospho- and total NF-κB inducing kinase (NIK). BCL10 was silenced by siRNA and effects of mutations of specific phosphorylation sites of BCL10 (Ser138Gly and Ser218Gly) were determined.

Results: By the non-canonical pathway, LPS exposure increased nuclear RelB and p52, and phospho-NIK, with no change in total NIK. Phosphorylation of BCL10 Serine 138 was required for NIK phosphorylation, since mutation of this residue eliminated the increases in phospho-NIK and nuclear RelB and p52. Mutations of either Serine 138 or Serine 218 reduced RelA, p50, and phospho-IκBα of the canonical pathway. Effects of LPS stimulation and BCL10 silencing on NIK phosphorylation were demonstrated in confocal images.

Conclusions: LPS-induces activation of both canonical and non-canonical pathways of NFκB in human colonic epithelial cells, and the non-canonical pathway requires phosphorylations of BCL10 (Serine 138) and NIK. These findings demonstrate the important role of BCL10 in mediating LPS-induced inflammation in human colonic epithelial cells and may open new avenues for therapeutic interventions.

258 words

Key Words: Lipopolysaccharide; BCL10; IKK signalosome; NF-κB

Introduction

Lipopolysaccharide (LPS), a structural component of the outer envelope of all gram-negative bacteria, has three distinct domains. These include: 1) the highly conserved Lipid A domain composed of a phosphorylated glucosamine disaccharide backbone with multiple hydrophobic fatty acids; 2) a core oligosaccharide attached to Lipid A; and 3) the O-antigen, a variable polysaccharide side chain that extends from the core oligosaccharide and confers antigenic specificity to LPS from different bacteria. LPS is released into the circulation from the surface of gram-negative bacteria, alone or in association with other endogenous factors, and induces an intense inflammatory response, mediated by the toll-like receptor 4 (TLR4) in human colonic epithelial cells [1-5].

Nuclear Factor (NF)-κB is a key determinant of the intestinal epithelial inflammatory reactions in response to LPS and occupies a central role in the transcriptional activation of proinflammatory genes. The involvement of B-cell lymphoma/leukemia (BCL)-10 in the activation of NFκB has been very well documented in lymphocytes and macrophages, and translocations involving BCL10 are associated with the constitutive activation of NFκB in the MALT (mucosa-associated lymphoid tumor) lymphomas [6-10]. BCL10 has also been implicated in gastric stromal tumors, not associated with *Helicobacter pylori* [11,12]. BCL10, like nucleotide-binding oligomerization domain containing 2 (NOD2), which is an intracellular pattern recognition receptor protein that is associated with genetic predisposition to Crohn's Disease, has a caspase recruitment domain (CARD).

Recent studies have demonstrated that Bcl10 is a critical mediator in the activation of LPS, carrageenan, and platelet-activating factor (PAF)-induced inflammation in human colonic epithelial cells [13-15], angiotensin II-induced inflammation in hepatocytes [16],

lysophosphatidic acid-induced activation of NF-κB in murine embryonic fibroblasts [17], and G-protein-coupled receptor mediated activation of NF-κB in human embryonic 293 kidney cells [18]. Bcl10 has been identified by several different names in early reports, including CIPER, cCARMEN, c-E10, mE10, and hCLAP [19]. Previously, we reported that LPS activated NF-κB by two distinct pathways in human colonic epithelial cells: a toll-like receptor (TLR)-4-BCL10 pathway and a reactive oxygen species (ROS)-Heat shock protein (Hsp)27 pathway [20]. These cascades were integrated at the level of the IκB kinase (IKK) signalosome, leading to the phosphorylation and ubiquitination of IκBα and the nuclear translocation of NF-κB p65. LPS stimulated both of these pathways in the human and mouse tissues and cell lines that were studied, and the complete abrogation of NF-κB p65 activation required inhibition of both cascades.

The non-canonical pathway of NFκB activation, when elucidated in relation to TNFα, involved stimulation through the TNF-receptor with subsequent effects on TNF-receptor associated factors (TRAFs), including the ubiquitination of TRAF2. Reactions proceeded to induce increased NFκB-inducing kinase (NIK), phosphorylation of IκB-inducing kinase (IKK)-α, and NFκB cytoplasmic processing leading to the nuclear translocation of RelB and p52. These latter steps contrast with the canonical (RelA) activation that involves IKKβ phosphorylation, leading to the phosphorylation and subsequent ubiquitination of IκBα, and the nuclear translocation of RelA (p65) and p50 [21-23].

Previously, LPS was implicated in NFκB activation by the non-canonical pathway, as well as the canonical pathway, but the mechanism by which this proceeded was not precisely clarified, since LPS produced no increase in total NIK, and an effect of LPS on phospho-NIK has not previously been demonstrated [24,25]. In this report, we present new findings that

demonstrate LPS activation of the non-canonical pathway of NFκB activation in human colonic epithelial cells, leading to increased nuclear RelB and p52. This cascade involves phosphorylations of BCL10 Ser 138 and NFκB-inducing kinase (NIK). By studies in mouse embryonic fibroblasts (MEF), in which either IKKα or IKKβ has been selectively knocked out, distinct LPS effects mediated by either IKKα or IKKβ are defined. Since endotoxin has such a critical role in sepsis and in the systemic inflammatory response syndrome, these findings may lead to new approaches to prevention and treatment of LPS-induced morbidity and mortality, as well as to increased understanding of mechanisms of intestinal inflammation.

Materials and Methods

Cell Culture

NCM460 is a nontransfected human colonic epithelial cell line, originally derived from the normal colonic mucosa of a 68-year-old Hispanic male. NCM460 cells were obtained and expanded in M3:10 media (INCELL, San Antonio, TX) [26]. The cells were maintained at 37°C in a humidified, 5% CO_2 environment with media exchanges at two day intervals. Confluent cells in T-25 flasks (Costar, Cambridge, MA) were harvested by trypsinization and subcultured in multiwell tissue culture clusters (Costar). Cells were treated with LPS (10 ng/ml; Sigma Chemical Company, St. Louis, MO) for 6 hours. At the end of the treatment, the spent media were collected from control and treated wells and stored at -80°C until further analysis. Cells were harvested by scraping, and cell lysates were prepared and stored at -80°C. Total cell protein was measured by BCA protein assay kit (Pierce, Rockford, IL), using bovine serum albumin as the standard.

Mouse embryonic fibroblasts (MEF), including wild type (WT), IKK$\alpha^{-/-}$ and IKK$\beta^{-/-}$ were a generous gift from Dr. Michael Karin's laboratory (University of California, San Diego). These cell lines were developed from transgenic homozygous mice in which IKKα and IKKβ genes were deleted [27]. The WT, IKK$\alpha^{-/-}$ and IKK$\beta^{-/-}$ cells were grown in Dulbecco's modified Eagle's medium with 10% fetal bovine serum. The cells were maintained and treated with LPS, using similar procedures as with the NCM460 cells.

Inhibition of TLR4-mediated pathway by blocking antibody

NCM460 cells were grown in 12-well tissue culture plates. When 70 - 80% confluent, the cells were treated for 2 h with fresh media containing 20 μg/ml TLR4 receptor-blocking antibody (HTA-125; BioLegend, San Diego, CA) or IgG2α prior to LPS exposure for 6 h. Cells were

incubated at 37°C in a humidified 5% CO_2 environment. After 6h, the extent of NIK phosphorylation was determined by FACE assay (see below).

BCL10 mRNA Silencing

Small interfering (si) RNA for BCL10 was procured (Qiagen, Valencia, CA), and BCL10 expression was silenced as described previously [13]. Cells were grown to 60-70% confluency in 12-well tissue culture plates, and the medium of the growing cells was aspirated and replaced with 1.1 ml of fresh medium with serum. 0.3µl of 20µM siRNA (75 ng) was mixed with 100µl of serum-free medium and 6µl of HiPerfect Transfection Reagent (Qiagen). The mixture was incubated at room temperature for 10 minutes to allow the formation of transfection complexes, then added dropwise onto the cells. The plate was swirled gently, and treated cells were incubated at 37°C in a humidified 5% CO_2 environment. After 24 hours, the medium was exchanged with fresh growth medium. Effectiveness of Bcl10 silencing in the NCM460 cells and the MEF was demonstrated previously by ELISA [13,28,29]**.**

The secretion of IL-8 in the spent medium of control and treated NCM460 cells was measured by a commercial ELISA kit for human IL-8 (R&D Systems, Minneapolis, MN), as described previously [13]**.** KC, the mouse homolog of IL-8, was measured in the spent medium of embryonic fibroblasts by a commercial ELISA (R&D Systems) [13]. Values were extrapolated from standard curves and normalized by the total cell protein concentrations, and expressed as pg/mg protein.

Expression of BCL10 protein in control and LPS-treated NCM460 and embryonic fibroblasts was determined by a solid-phase ELISA, previously developed by our laboratory for quantitative determination of BCL10 [28]**.** Control or treated cells were lysed in RIPA buffer (50

mM Tris containing 0.15 M NaCl, 1% Nonidet P-40,0.5% deoxycholic acid, and 0.1% SDS, pH 7.4), and the cell extracts were stored at -80 °C until assayed by the ELISA.

Phosphorylation of IκBα was determined using a PathScan Sandwich ELISA kit (Cell Signaling Technology, Danvers, MA) [14, 30]**.** Briefly, IκBα in the cell extracts was captured in a 96- well ELISA plate that was pre-coated with mouse monoclonal antibody against human and mouse IκBα. Phosphorylation was determined by a phospho-IκBα antibody [Ser32, Santa Cruz Biotechnology (SCBT), Santa Cruz, CA], and detection was by an HRP-conjugated secondary antibody and measurement of the hydrogen peroxide-tetramethylbenzidine (TMB) chromogenic substrate

ELISA for Measurement of RelA, RelB, p50, and p52

Nuclear extracts were prepared from treated and control cells using a nuclear extraction kit (Active Motif, Carlsbad, CA). Activated NFκBs (RelA, RelB, p52, or p50) in the samples were measured by oligonucleotide-based ELISA (Active Motif) [29]**.** Treated and control samples were incubated in wells of a 96-well microtiter plate that were coated with the NF-κB consensus nucleotide sequence (5-GGGACTTTCC-3). NF-κB from the cell samples attached to the wells and was captured by specific antibody to either RelA, RelB, p50, or p52. Binding of the specific NFκB family member was then detected by an anti-rabbit-HRP-conjugated IgG. Color developed with hydrogen peroxide/TMB chromogenic substrate, and intensity of the developed color was proportional to the quantity of RelA, RelB, p50, or p52 in each sample. The specificity of the binding to the nucleotide sequence was ascertained by pre-mixing of either free consensus nucleotide or mutated nucleotide to the sample before adding the cell preparation to the well. Sample determinations were normalized by the total cell protein, as determined by protein assay

kit (Pierce). Data were expressed as % untreated control. In the IKK cells, the percentages in the IKK$\alpha^{-/-}$or IKK$\beta^{-/-}$ cells are calculated in relation to the values in the WT cells.

Measurement of phospho-BCL10 by FACE Assay

Phosphorylation of BCL10 in control and LPS-treated cells was measured by a fast-activated cell-based (FACE) ELISA (Active Motif) [29]**.** Control and treated cells were fixed with 4% formaldehyde and then washed. Cellular peroxide activity was quenched by addition of quenching buffer that contains PBS with H_2O_2, and the non-specific binding was blocked by blocking buffer (Active Motif). Phospho-BCL10 was captured by a specific monoclonal phospho-BCL10 antibody (Ser138, sc-81484; Santa Cruz Biotechnology (SCBT), Santa Cruz, CA), and detected by anti-mouse-IgG-HRP (SCBT) and hydrogen peroxide-TMB substrate.

Measurement of phospho-NIK by FACE Assay

Total and phospho-NIK in control and LPS-treated NCM460 and embryonic fibroblasts were measured by FACE ELISA (Active Motif) [29]. A primary rabbit polyclonal antibody for NIK [sc-7211; SCBT] against the epitope AA:700-947 and a primary polyclonal goat antibody for phospho-NIK (sc-12957; SCBT) that recognized Thr^{559} phosphorylation were used to determine the extent of NIK phosphorylation. Measurements of optical density were compared between control and treated samples and the data are expressed as % control.

Site-directed mutagenesis

To ascertain the role of serine-138 and serine-218 of the Bcl10 protein in mediating its functional effects, site-directed mutagenesis was performed to generate mutant Bcl10 proteins, in which one of the serine residues was changed to glycine (S138G or S218G), using the QuickChange Site Directed Mutagenesis Kit (Stratagene, La Jolla, CA), according to the manufacturer's instructions. Mutations were confirmed by sequencing. The following mutant

oligonucleotides were used to insert the mutations (underlined letters indicate mutated residues): for M1 (S138G), 5′-CTCTCCAGATCAAAT**GG**AGATGAGAGTAATTTC-3′; for M2 (S218G), 5′-GGAACTTGTGCAAAC**GG**TAGTGAGATGTTTCTT-3′.

Confocal microscopy for imaging of NIK and phospho-NIK

NCM460 cells were grown in four-chamber tissue culture slides for 24h, and then treated with LPS 10 ng/ml for 6h. Methods for staining and examining cells by confocal microscopy were described previously [30]**.** Cells were washed once in 1×phosphate-buffered saline (PBS) containing 1 mM calcium chloride (pH 7.4), fixed for 1.5 h with 2% paraformaldehyde, and then permeabilized with 0.08% saponin. Preparations were washed with PBS, blocked by 5% normal goat serum, incubated overnight with NIK or p-NIK antibody (SCBT), and then washed and stained with either goat anti-rabbit Alexa Fluor® IgG 568 (for NIK) or donkey anti-goat Alexa Fluor® IgG 568 (for p-NIK), as well as phalloidin-Alexa Fluor® 488 (Invitrogen) for 1 hour. Preparations were washed thoroughly and mounted with mounting medium containing DAPI (Vectashield®, Vector Laboratories, Inc., Burlingame, CA) for nuclear DNA staining, and observed using a Zeiss LSM 510 laser-scanning confocal microscope. Excitation was at 488 and 534 nm from an argon/krypton laser and at 361 nm from a UV laser. Green and red fluorescence were detected through LP505 and 585 filters. The fluorochromes were scanned sequentially, followed by export of the collected images using Zeiss LSM Image Browser software for analysis and reproduction.

Statistics

Data presented are the mean ± standard deviation (SD) of at least three biological samples with technical replicates of each sample. Unless stated otherwise in the text or figure legend, statistical significance was determined by one way analysis of variance (ANOVA),

followed by a post-hoc Tukey–Kramer test for multiple comparisons using InStat3 software (GraphPad, La Jolla, CA). A p-value ≤ 0.05 is considered statistically significant. In the figures, *** indicates $p<0.001$, ** $p<0.01$, and * $p<0.05$. Error bars indicate SD.

Results

LPS-induced increases in nuclear RelA, RelB, p50, and p52 were reduced by silencing BCL10 in human colonic epithelial cells

NCM460 cells were exposed to LPS from *E. coli* (10 ng/ml x 6 hours), and effects on nuclear NF-κB family members RelA (p65), RelB, p50, and p52 were measured. LPS increased both nuclear RelA and RelB, to 3.8 and 1.8 times the baseline values, respectively ($p<0.001$) (**Fig. 1A**). BCL10 silencing reduced the LPS-induced increase in RelA (to 2.2 times baseline) and eliminated the increase in RelB completely ($p<0.001$). Corresponding to the change in RelA, p50 increased to 3.9 times baseline and declined to 2.2 times baseline following BCL10 silencing. In parallel fashion, changes in p52 corresponded to those in RelB, increasing to two times baseline with LPS exposure, and returning to baseline wihen BCL10 was silenced. These results demonstrate that BCL10 is required for LPS-induced effects on mediators of both canonical (RelA and p50) and non-canonical (RelB and p52) pathways of NFκB acdtivation..

Differential effects of Bcl10 silencing on NFκB family members in WT, IKKα$^{-/-}$, and IKKβ$^{-/-}$ MEF

Differential effects of LPS and of Bcl10 silencing on RelA, RelB, p50, and p52 occurred in the mouse embryonic fibroblasts (MEF). Treatment of MEF wild type (WT) and IKKα$^{-/-}$ cells with LPS increased the nuclear content of RelA, to 4.0 and 3.2 times the baseline values, respectively ($p<0.001$) (**Figs. 1B, 1C**). As in the NCM460 cells, Bcl10 silencing markedly reduced the LPS-induced increases in nuclear RelA, to 2.2 times the baseline level in the WT MEF and to 1.9 times the baseline in the IKKα$^{-/-}$ cells ($p<0.001$). Similar effects occurred in nuclear p50.

In contrast, LPS exposure did not increase nuclear RelA or p50 in the IKKβ$^{-/-}$ cells, but RelB and p52 both increased to ~two times the baseline value ($p<0.001$) (**Fig. 1D**). Bcl10 silencing completely inhibited the LPS-induced increase in nuclear RelB and p52 in the IKKβ$^{-/-}$ cells.

In the IKKα$^{-/-}$ cells, LPS did not induce an increase in RelB or p52 (**Fig. 1C**). RelB and p52 increased to ~two times the baseline level in the WT MEF cells, and these increases were completely inhibited by Bcl10 knockdown by siRNA (**Fig. 1B**), as in the IKKβ$^{-/-}$ cells. These findings demonstrate dependence on the presence of IKKα, and are consistent with the involvement of IKKα in the non-canonical pathway.

LPS exposure increased phospho-NIK, but not total NIK

Treatment of NCM460 cells with LPS produced no significant changes in total NIK, but phospho-NIK increased from 9.2 ± 0.1% of the total NIK to 36.2 ± 3.0% of the total NIK ($p<0.001$) (**Fig. 2A**). Bcl10 silencing by siRNA reduced the LPS-induced increase in phospho-NIK to baseline level. The LPS-induced increase in phospho-NIK in the NCM460 cells was totally blocked when the cells were treated with TLR4 blocking antibody for 2 hours before LPS exposure, consistent with LPS activation of the non-canonical pathway through TLR4 (data not shown).

Similarly, in the WT MEF cells, total NIK did not change following exposure to LPS, but phospho-NIK increased from 8.9 ± 0.6% of the total NIK to 32.1 ± 1.7% of the total NIK ***(*Fig. 2B*)***. Also, in the MEF IKKα$^{-/-}$ cells, phospho-NIK increased from 8.3 ± 0.9% to 30.1 ± 1.9% of the total NIK (**Fig. 2C)**, and from 9.1 ± 0.8% to 31.0 ± 2.5% of the total NIK in the MEF IKKβ$^{-/-}$ cells (**Fig. 2D)**. These findings indicate that the LPS-induced increase in phospho-NIK must

occur upstream of the IKK signalosome, since phospho-NIK content was unaffected by the presence or absence of IKKα or IKKβ.

Confocal images of total NIK and phospho-NIK following LPS and BCL10 silencing in NCM460 cells

Confocal microscopy of total NIK (**Fig. 3, A–F**) and phospho-NIK (**Fig. 4, A-F**) in NCM460 cells supported the finding that LPS-induced NIK phosphorylation was BCL10-dependent. Staining for phospho-NIK was absent when BCL10 expression was silenced by specific siRNA. In contrast, total NIK staining did not change after LPS exposure, nor after BCL10 silencing.

Mutation of Serine 138 of BCL10 inhibited LPS-induced increases in Phospho-NIK and RelB , but not in RelA in NCM460 cells

Silencing BCL10 expression eliminated the LPS-induced increases in phospho-NIK in the NCM460 cells (**Fig. 2A**) and in the MEF (**Figs. 2B-D**), demonstrating a requirement for BCL10. In order to demonstrate how BCL10 might lead to NIK phosphorylation, NCM460 cells were transfected with either wild type BCL10 or BCL10 mutated at Ser138 or at Ser218 and treated with LPS (10 ng/ml x 6 h). Phospho-BCL10 (Ser 138) was measured to determine the effectiveness of the Ser138Gly mutation (**Fig. 5A**). When transfected with wild type BCL10 and exposed to LPS, phospho-Ser increased to 7.0 times the control phospho-BCL10 (Ser 138) level. Cells transfected with the Ser138Gly mutant showed a decline in the measured phospho-BCL10. In contrast, cells transfected with the Ser218Gly mutant demonstrated an increase in phospho-BCL10 similar to that following transfection with wild type BCL10.

In NCM460 cells transfected with mutated BCL10 (Ser138Gly), no increase in phospho-NIK occurred, in contrast to increases in phospho-NIK in cells transfected with either wild type

BCL10 (to 376 ± 27% of the baseline) or the Ser218Gly mutant (to 413 ± 18% of the baseline) (**Fig. 5B**). These findings indicate a selective effect of BCL10 Ser138 on NIK phosphorylation and, thereby, on the non-canonical pathway.

LPS treatment of NCM460 cells transfected with either wild type or mutated BCL10 produced an increase in nuclear RelA in the cells transfected with wild type BCL10 to 3.9 ± 0.1 times the baseline (**Fig. 5C**).RelA increased to ~2 times the baseline value in the cells transfected with either the Ser138Gly (to 2.2 ± 0.3) or Ser218Gly (to 2.0 ± 0.2) mutants. These findings demonstrate the importance of both Ser138 and Ser218 in the activation of RelA.

In contrast, LPS produced a smaller increase in RelB, and this increase was completely absent in the Ser138Gly mutant cells (**Fig. 5D**). Nuclear RelB in the NCM460 cells transfected with either wild type BCL10 or the Ser218Gly mutant increased to ~1.8 times the baseline level. These findings are consistent with the impact of the Ser138Gly mutation on phospho-NIK, and on activation of the non-canonical pathway.

BCL10 mutations or silencing reduced the LPS-induced increases of phospho-IκBα and IL-8 or KC

NCM460 cells transfected with either wild type or Ser138 or Ser218 mutant BCL10 were treated with LPS, and the phospho-IκBα content (**Fig. 6A**) and IL-8 secretion (**Fig. 6B**) were measured. LPS treatment of NCM460 cells transfected with either wild type or mutated BCL10 demonstrated increased phosphorylation of IκBα. In the wild type cells, phosphorylation of IκBα increased to ~3.9 times the baseline; in the mutated cells, phospho-IκBα increased to ~ 2.2 times the baseline value.

Secreted IL-8 increased from baseline of 215 ± 11 pg/mg protein to 3144 ± 204 pg/mg protein. Cells transfected with either of the BCL10 mutants also demonstrated increases in IL-8

secretion after LPS treatment, but the increases were ~60% less in the mutants, compared to the wild type BCL10.

LPS treatment induced the phosphorylation of IκBα in MEF WT and IKKα$^{-/-}$, but not in IKKβ$^{-/-}$ cells (**Fig. 6C**), consistent with the lack of involvement of IKKα in the canonical pathway of NFκB activation. Phosphorylation of IκBα increased to 3.8 ± 0.3 times the baseline value in the MEF WT and to 2.7 ± 0.5 times the baseline in the IKKα$^{-/-}$ cells. These increases were partially reduced by BCL10 silencing or by Tempol ($p<0.001$), and completely inhibited by their combination (data not shown). In contrast, in the IKKβ$^{-/-}$ cells, phospho-IκBα did not increase following LPS exposure, indicating the presence of a phospho-IκBα independent pathway of KC activation by LPS, mediated through IKKα.

In wild type MEF, the KC secretion increased to 5.2 ± 0.4 times the baseline, following exposure to LPS (10 ng/ml x 6 hours). In contrast, in the IKKα$^{-/-}$ and IKKβ$^{-/-}$ cells, KC secretion increased to 3.5 ± 0.3 and 1.9 ± 0.1 times the baseline, respectively (**Fig. 6D)**. Silencing Bcl10 expression by siRNA significantly reduced the LPS-induced increases in KC secretion in the MEF cells. The LPS-induced increase in KC secretion was eliminated in the IKKβ$^{-/-}$ cells after Bcl10 silencing. The reactive oxygen species quencher Tempol in combination with Bcl10 siRNA eliminated the LPS-induced increases in KC in the MEF WT and IKKα$^{-/-}$ cells, but had no additional effect in the IKKβ$^{-/-}$ cells (data not shown).

Discussion

This study expands our understanding of how BCL10 mediates the activation of the non-canonical pathway of NFκB activation, by showing that stimulation of RelB and p52 by LPS requires phosphorylation of BCL10. LPS-induced increases in phospho-NIK and RelB were inhibited by silencing BCL10, and mutation of serine 138 of BCL10 inhibited the phosphorylation of NIK. The LPS-induced noncanonical pathway required activation of both BCL10 and NIK by phosphorylation. Previously, no change in NIK post LPS treatment was reported [24], and it was concluded that LPS was not associated with activation of the non-canonical pathway. However, other reports suggested that LPS did activate the non-canonical pathway [31,32]. Our results demonstrate no increase in total NIK, but indicate that LPS can activate the non-canonical pathway by phosphorylation of NIK, and that this phosphorylation requires prior phosphorylation of Ser138 of BCL10. The pathways are depicted in **Figure 7,** and resemble the recently reported carrageenan-associated pathways [29]. Importantly, additional findings in this report specify the effects of distinct mutations in BCL10 on LPS-induced effects involving phospho-NIK, RelA, RelB, IL-8, and phospho-IκBα.

Activation of NIK by phosphorylation has been reported in other studies [33,34]**.** These effects occur upstream of the IKK signalosome, consistent with our findings, since responses to LPS were similar in the MEF IKKα$^{-/-}$ and IKKβ$^{-/-}$ cells. Following LPS interaction with TLR-4, activation of BCL10, involving phosphorylations at serines 138 and 218, appeared to enable the phosphorylation of NIK to phospho-NIK. Independently of the IKK signalosome and of phospho-IκBα, LPS, by this pathway, induces translocation of RelB and p52 into the nucleus, in order to influence the transcription of inflammatory genes, such as IL-8, and innate immune responses.

By induction of both the canonical and noncanonical pathways of NF-κB activation, LPS influences a wider range of NF-κB transcriptional events [35-37]**.** LPS is one of the few known inducers of both the noncanonical and canonical pathways of NF-κB activation, a group that includes lymphotoxin, B-cell activating factor (BAFF), and carrageenan [20,38,39]. This study, to the best of our knowledge, is the first report of a mechanism by which LPS activates the non-canonical pathway in non-myeloid cells.

The non-canonical pathway of NF-κB has been identified as an alternate route by which transcription of genes involved in inflammation can be regulated. Reports have suggested complex feedback between the canonical and non-canonical pathways and the potential of the non-canonical pathway to provide a more sustained activation of specific genes [35-37]. Hence, the ability of LPS to activate both RelA and RelB confers additional avenues by which the impact of LPS exposure on vital cellular processes can be transmitted. Also, demonstration that BCL10 is involved in both canonical and non-canonical pathways increases considerations about the important role of BCL10 in mediating inflammation and the innate immune response [40].

LPS is a significant source of clinical morbidity and mortality owing to its role in the etiology of systemic inflammatory response syndrome (SIRS) and sepsis. Although improvements in the therapeutic approach to SIRS and sepsis have been achieved, better understanding of the underlying mechanisms by which LPS induces inflammation may improve clinical outcomes and lead to new approaches to treatment. Recognition of the impact of LPS exposure on both the canonical and non-canonical pathways of NF-κB activation and of the role of BCL10 in these cascades may lead to new insights into how to reverse or prevent harmful inflammatory effects initiated by LPS present in the colonic microflora.

References

1. Bocker U, Yezerskyy O, Feick P, Manigold T, Panja A, Kalina U, Herweck F, Rossol S, Singer MV. Responsiveness of intestinal epithelial cell lines to lipopolysaccharide is correlated with Toll-like receptor 4 but not Toll-like receptor 2 or CD14 expression. Int J Colorectal Dis 2003;18:25-32.
2. Medzhitov R, Janeway C. The Toll receptor family and microbial recognition. Trends Microbiol 2000;8:452-456.
3. Arbour NC, Lorenz E, Schutte BC, Zabner J, Kline JN, Jones M, Frees K, Watt JL, Schwartz DA. TLR4 mutations are associated with endotoxin hyporesponsiveness in humans. Nat Genet 2000;25:187-191.
4. Raetz CR, Whitfield C. Lipopolysaccharide endotoxins. Annu Rev Biochem 2002;71: 635-700.
5. Hornef MW, Normark BH, Vandewalle A, Normark S. Intracellular recognition of lipopolysaccharide by toll-like receptor 4 in intestinal epithelial cells. J Exp Med 2003;198:1225-1235.
6. Sun L, Deng L, Ea CK, Xia ZP, Chen ZJ. The TRAF6 ubiquitin ligase and TAK1 kinase mediate IKK activation by BCL10 and MALT1 in T lymphocytes. Mol Cell 2004;14: 289-301.
7. Zhang Q, Siebert R, Yan M, Hinzmann B, Cui X, Xue L, Rakestraw KM, Naeve CW, Beckmann G, Weisenburger DD, Sanger WG, Nowotny H, Vesely M, Callet-Bauchu E, Salles G, Dixit VM, Rosenthal A, Schlegelberger B, Morris SW. Inactivating mutations and overexpression of BCL10, a caspase recruitment domain-containing gene, in MALT lymphoma with t(1;14)(p22;q32). Nat Genet 1999;22:63-68.

8. Willis TG, Jadayel DM, Du MQ, Peng H, Perry AR, Abdul-Rauf M, Price H, Karran L, Majekodunmi O, Wlodarska I, Pan L, Crook T, Hamoudi R, Isaacson PG, Dyer JF. BCL10 is involved in t(1;14)(p22;q32) of MALT B Cell lymphoma and mutated in multiple tumor types. Cell 1999;96**:**46-56.

9. Wu CJ, Ashwell JD. NEMO recognition of ubiquitinated Bcl10 is required for T cell receptor-mediated NF-κB activation. Proc Natl Acad Sci U S A 2008;105:3023-3028.

10. Zhou, H., Wertz, I., O'Rourke, K., Ultsch, M., Seshagiri, S., Eby, M., Xiao, W., and Dixit, V. M. Bcl10 activates the NFκB pathway through ubiquitination of NEMO. Nature 2004;427,167-171.

11. Kuo SH, Chen LT, Wu MS, Kuo KT, Yeh KH, Doong SL, Yeh PY, Hsu HC, Tzeng YS, Lin CW, Lin JT, Cheng AL. Differential response to H. pylori eradication therapy of co-existing diffuse large B-cell lymphoma and MALT lymphoma of stomach-significance of tumour cell clonality and BCL10 expression. J Pathol 2007; 211(3):296-304.

12. Ye H, Gong L, Liu H, Ruskone-Fourmestraux A, de Jong D, Pileri S, Thiede C, Lavergne A, Boot H, Caletti G, Wündisch T, Molina T, Taal BG, Elena S, Neubauer A, Maclennan KA, Siebert R, Remstein ED, Dogan A, Du MQ. Strong BCL10 nuclear expression identifies gastric MALT lymphomas that do not respond to H pylori eradication. Gut 2006; 55(1):137-8.

13. Borthakur A, Bhattacharyya S, Dudeja PK, Tobacman JK. Carrageenan induces Interleukin-8 production through distinct Bcl10 pathway in normal human colonic epithelial cells. Am J Physiol Gastrointest Liver Physiol 2007;292:G829–G838.

14. Borthakur A, Bhattacharyya S, Alrefai W, Tobacman JK, Ramaswamy K, Dudeja PK. Bcl10 mediates LPS-induced activation of NF-kappaB and IL-8 in human intestinal epithelial cells. Am J Physiol Gastrointest Liver Physiol 2007; 293(2):G429-G437.

15. Borthakur A, Bhattacharyya S, Alrefai W, Tobacman JK, Ramaswamy K, Dudeja PK. Platelet-activating factor-induced NF-κB activation and IL-8 production in intestinal epithelial cells are Bcl10 dependent. Inflamm Bowel Dis 2009 Aug 27 [Epub ahead of print]

16. McAllister-Lucas LM, Ruland J, Siu K, Jin X, Gu S, Kim DS, Kuffa P, Kohrt D, Mak TW, Nunez G, Lucas PC. CARMA3/Bcl10/MALT1-dependent NFkappaB activation mediates angiotensin II-responsive inflammatory signaling in nonimmune cells. Proc Natl Acad Sci USA 2007;104:139-144.

17. Klemm S, Zimmermann S, Peschel C, Mak TW, Ruland J. Bcl10 and Malt1 control lysophosphatidic acid-induced NF-κB activation and cytokine production. Proc Natl Acad Sci USA 2007;104: 134-138.

18. Wang D, You Y, Lin PC, Xue L, Morris SW, Zeng H, Wen R, Lin X. Bcl10 plays a ritical role in NF-κB activation induced by G protein-coupled receptors. Proc Natl Acad Sci USA 2007;104:145–150.

19. http://www.ncbi.nlm.nih.gov/protein?term=Bcl10

20. Bhattacharyya S, Dudeja PK, Tobacman JK. Lipopolysaccharide activates NF-kappaB by TLR4-Bcl10-dependent and independent pathways in colonic epithelial cells. Am J Physiol Gastrointest Liver Physiol 2008; 295(4):G784-G790.

21. Häcker H, Karin M. Regulation and function of IKK and IKK-related kinases. Sci. STKE 2006;357: re13.

22. Grech AP, Amesbury M, Chan T, Gardam S, Basten A, Brink R. TRAF2 differentially regulates the canonical and noncanonical pathways of NF-kappaB activation in mature B cells. Immunity 2004;21(5):629-642.

23. Bonizzi G, Karin M. The two NF-kappB activation pathways and their role in innate and adaptive immunity. Trends Immunol 2004;25(6):280-288.

24. Smith C, Andreakos E, Crawley JB, Brenna FM, Feldmann M, Foxwell BM. NF-kappaB-inducing kinase is dispensable for activation of NF-kappaB in inflammatory settings but essential for lymphotoxin beta receptor activation of NF-kappaB in primary fibroblasts. J Immunol 2001;167(1):5895-903.

25. Andreakos E, Smith C, Monaco C, Brenna FM, Foxwell BM, Feldmann M. IkappaB kinase 2 but not NF-kappaB-inducing kinase is essential for effective DC antigen presentation in the allogeneic mixed lymphocyte reaction. Blood 2003;101(3):983-91.

26. Moyer M.P**,** Manzano LA, Merriman RL, Stauffer JS, Tanzer LR. NCM460, a normal human colon mucosal epithelial cell line. In Vitro Cell Dev Biol Anim 1996;32:315-317.

27. Hu Y, Baud V, Delhase M, Zhang P, Deerinck T, Ellisman M, Johnson R, Karin M. Abnormal morphogenesis but intact IKK activation in mice lacking the IKKα subunit of the IκB kinase. Science 1999;294:316-320.

28. Bhattacharyya S, Pant N, Dudeja PK, Tobacman JK. Development, evaluation, and application of a highly sensitive microtiter plate ELISA for human Bcl10 protein. J Immunoassay Immunochem 2007;28(3):173-188.

29. Bhattacharyya S, Borthakur A, Tyagi S, Gill R, Chen ML, Dudeja PK, Tobacman JK. B-cell CLL/lymphoma 10 (BCL10) is required for NF-kappaB production by both

canonical and noncanonical pathways and for NF-kappaB-inducing kinase (NIK) phosphorylation. J Biol Chem 2010;285(1):522-530.

30. Bhattacharyya S, Gill R, Chen ML, Zhang F, Linhardt RJ, Dudeja PK, Tobacman JK Toll-like Receptor 4 Mediates Induction of BCL10-NFκB-IL-8 Inflammatory Pathway by Carrageenan in Human Intestinal Epithelial Cells. J Biol Chem 2008;283:10550-10558.

31. Souvannavong V, Saidji N, Chaby R. Lipopoysaccharide from *Salmonella enterica* activates NF-kappaB through both classical and alternative pathways in primary B lymphocytes. Infect Immun 2007;75(10):4998-5003.

32. Hofer S, Rescigno M, Granucci F, Citterio S, Francolini M, Ricciardi-Castagnoli P. Differential activation of NF-kappaB subunits in dendritic cells in response to gram-negative bacteria and to lipopoysaccharide. Microbes Infect.2001;3(4):259-265.

33. Rangaswami H, Bulbule A, Kundu GC. Nuclear factor-inducing kinase plays a crucial role in osteopontin-induced MAPK/IκBα kinase-dependent nuclear factor κB-mediated promatrix metalloproteinase-9 activation. J Biol Chem 2004;279(37):38921-38935.

34. Je JH, Lee JY, Jung KJ, Sung B, Go EK, Yu BP, Chung HY. NF-κB activation mechanism of 4-hydroxyhexenal via NIK/IKK and p38 MAPK pathway. FEBS Letters 2004;566:183-189.

35. Wharry CE, Haines KM, Carroll RG, May MJ. Constitutive non-canonical NFkappaB signaling in pancreatic cancer cells. Cancer BiolTher 2009;8:1567–1576.

36. Fusco AJ, Huang DB, Miller D, Wang VY, Vu D, Ghosh G. NF-κB p52:RelB heterodimer recognizes two classes of κB sites with two distinct modes. EMBO Rep 2009;10:152-159.

37. Dejardin E. The alternative NF-kappaB pathway from biochemistry to biology: pitfalls and promises for future drug development. Biochem Pharmacol 2006;72;1161-1179.

38. Yilmaz ZB, Weih DS, Sivakumar V, Weih F. RelB is required for Peyer's patch development: differential regulation of p52-RelB by lymphotoxin and TNF. EMBO J 2003; 22:121–130.

39. Endo T, Nishio M, Enzler T, Cottam HB, Fukuda T, James DF, Karin M, Kipps T. BAFF and APRIL support chronic lymphocytic leukemia B-cell survival through activation of the canonical NF-κB pathway. Blood 2007;109:703–710.

40. Li Z, Wang H, Xue L, Shin D-M, Roopenian D, Xu W, Q, C-F, Sangster MY, Orihuela CJ, Tumanen E, Rehg JE, Cui X, Zhang Q, Morse HC III, Morris SW. Eμ-BCL10 mice exhibit constitutive activation of both canonical and non-canonical NF-κB pathways generating marginal zone (MZ) B-cell expansion as a precursor to splenic MZ lymphoma. Blood 2009;114(19):4158-4168.

Legends

Figure 1. LPS effects on RelA (p65), RelB, p50, and p52 are modified by silencing BCL10 by siRNA.

A. In NCM460 cells, LPS [10 ng/ml x 6 hours, (used in all experiments)] produced significant increases in RelA (p65), RelB, p50, and p52 ($p<0.001$), compared to baseline values in untreated cells (not shown) or cells exposed to control siRNA. The LPS-induced increase in RelA was reduced from 3.8 ± 0.3 times the baseline to 2.2 ± 0.1 times the baseline when BCL10 was silenced ($p<0.001$). With LPS stimulation, RelB increased to 1.8 ± 0.1 times the baseline, and declined to the baseline level when BCL10 was silenced ($p<0.001$). Changes in p50 and p52 correlated with the changes in RelA and RelB, respectively.[control si = control siRNA; LPS=lipopolysaccharide; BCL10 si = BCL10 siRNA]

B. In the WT MEF cells, RelA increased to 4.0 ± 0.2 times the baseline value following exposure to LPS, and this increase was reduced to 2.2 ± 0.03 times the baseline when Bcl10 was silenced. RelB increased to 2.0 ± 0.1 times the baseline and declined to baseline level following Bcl10 silencing ($p<0.001$). The changes in p50 and p52 were closely correlated with those in RelA and RelB, since p50 increased to 3.8 ± 0.2 times the baseline value, and declined to 2.2 ± 0.1 times the baseline when Bcl10 was silenced,and p52 increased to 2.0 ± 0.1 times the baseline value and returned to baseline following Bcl10 silencing.

C. In the IKK$\alpha^{-/-}$ cells, RelA increased to 3.2 ± 0.1 times the baseline and p50 increased to 3.2 ± 0.2 times the baseline following LPS. When Bcl10 was silenced, RelA increased to only 1.9 ± 0.1 times the baseline and p50 increased to only 1.8 ± 0.1 times the baseline ($p<0.001$). No increase in RelB or p52 occurred.

D. In the IKK$\beta^{-/-}$ cells, LPS exposure produced no increase in RelA or p50. In contrast, RelB increased to 2.0 ± 0.2 times the baseline and p52 increased to 2.0 ± 0.1 times the baseline, and both declined to baseline when Bcl10 was silenced ($p<0.001$).

Figure 2. LPS-induced increases in phospho-NIK are inhibited by BCL10 siRNA.

A. Following LPS exposure, phospho-NIK in the NCM460 cells increased from 9.4 ± 0.7% to 36.6 ± 0.3% of total NIK ($p<0.001$). This increase was suppressed by silencing BCL10.

B, C, and D. In the WT, IKK$\alpha^{-/-}$ and IKK $\beta^{-/-}$ MEF, total NIK did not change following LPS or Bcl10 silencing. In contrast, phospho-NIK increased to ~3.6 times the baseline value, and this increase was inhibited by silencing Bcl10.

Figure 3. Confocal imaging demonstrates no change in total NIK following LPS or BCL10 silencing.

In the images, green represents phalloidin-stained β-actin, red is total NIK, and blue is DAPI-stained DNA. A, C, and E demonstrate staining for total NIK; B, D, and F are the merged images.

A,B. Total NIK was stained in the NCM460 control cells.

C,D. Total NIK staining was not increased after LPS exposure and control siRNA.

E,F. Following BCL10 silencing, total NIK staining was similar to the control.

Figure 4. Confocal imaging demonstrates increase in phospho-NIK following LPS, but not when BCL10 is silenced by siRNA.

In the images of phospho-NIK (**A–F**), phalloidin-actin is stained green, DNA is stained blue, and phospho-NIK is stained red by Alexa-Fluor dyes, as described in the **Methods**. A, C, and E demonstrate staining for phospho-NIK; B, D, and F are the merged images.

A,B. No staining for phospho-NIK was seen in the control cells.

C,D. Following LPS exposure and control siRNA, phospho-NIK staining was increased significantly.

E,F. Following BCL10 silencing and LPS exposure, no staining for phospho-NIK was evident.

Figure 5. Mutation of BCL10 Serine 138, but not Serine 218, reduces phospho-NIK and RelB, but not RelA, in response to LPS.

A. When NCM460 cells were transfected with either wild type BCL10 or BCL10 mutants (Ser138Gly or Ser218Gly), the expected decline in phospho-BCL10, as measured by phospho-Ser138Gly, was evident in the Ser138Gly mutant. Transfections with both the wild type BCL10 and the Ser218Gly mutant produced marked increases in phospho-BCL10, expressed as % of control phospho-BCL10 ($p<0.001$).

B. Phospho-NIK increased to ~four times the baseline level, following transfections with the wild type BCL10 or Ser218Gly mutant, but there was no increase following transfection with the Ser138Gly mutant.

C. Transfections with wild type BCL10 and mutants (Ser138Gly and Ser218Gly) were all associated with increases in the LPS-induced nuclear RelA. Post LPS, RelA increased to ~3.9 times the baseline in the NCM460 cells transfected with wilt type BCL10 and to ~2 times the baseline in the cells transfected with the BCL10 mutants ($p<0.001$). Control was not exposed to LPS.

D. In contrast, transfection with the Ser138Gly BCL10 mutation abrogated the LPS-induced increase in RelB. RelB increased to ~1.8 times the baseline in the wild type BCL10 and Ser218Gly mutant.

Figure 6. Effects of BCL10 mutations on phospho-IκBα and IL-8 or KC.

A. Phospho-IκBα increased to ~3.9 times the baseline, following transfection with wild type BCL10 and stimulation by LPS. Both mutations reduced the increase in phospho-IκBα to ~2.2 times the baseline.

B. IL-8 increased to ~14.6 times the baseline level, following transfection with wild type BCL10 and LPS exposure (10 ng/ml x 6 hours). Both mutations reduced the LPS-induced increase in IL-8, to ~6.7 times the baseline.

C. In the IKKβ$^{-/-}$ MEF, no increase in phospho-IκBα followed LPS exposure, in contrast to the increases in the WT and IKKα$^{-/-}$ MEF.

D. In the IKKβ$^{-/-}$ MEF, the LPS-induced increase in KC was completely blocked by Bcl10 siRNA, in contrast to only partial inhibition in the WT and IKKα$^{-/-}$ MEF.

Figure 7. Schematic representation of LPS activation of RelA and RelB.

Three separate pathways of LPS-induced activation of NFκB are depicted, including a reactive oxygen species (ROS) pathway that requires Hsp27 and IKKβ, leading to increased RelA (p65). The canonical pathway of NFκB leads to increased RelA and proceeds through the IKK signalosome, involving phosphorylation and ubiquitination of IκBα. Both the canonical and the non-canonical pathways can be initiated through TLR-4. The non-canonical pathway proceeds through phospho-NIK, upstream of the IKK signalosome, and leads to increased RelB. BCL10 is required for both canonical and non-canonical pathways. IKKα does not participate in the LPS-induced activation of IκBα or RelA, and IKKβ does not participate in the LPS-induced activation of RelB.

Figure 1.

A

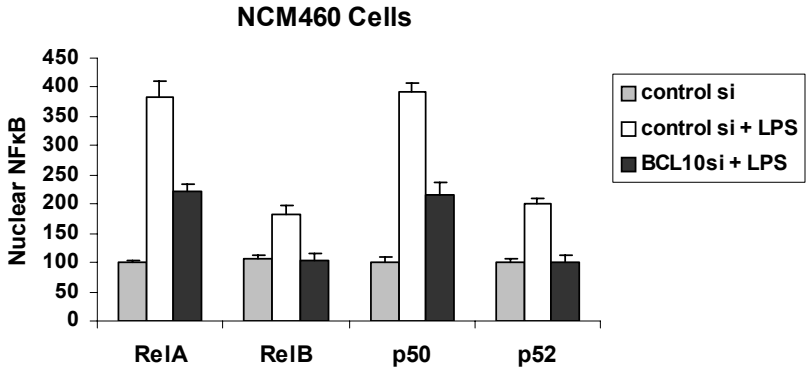

B

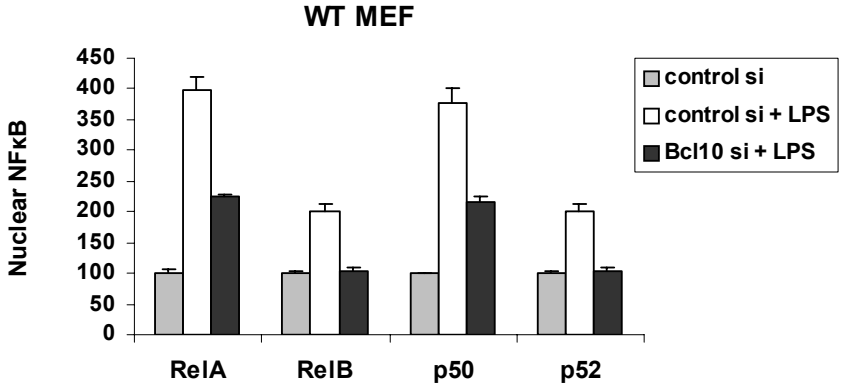

C

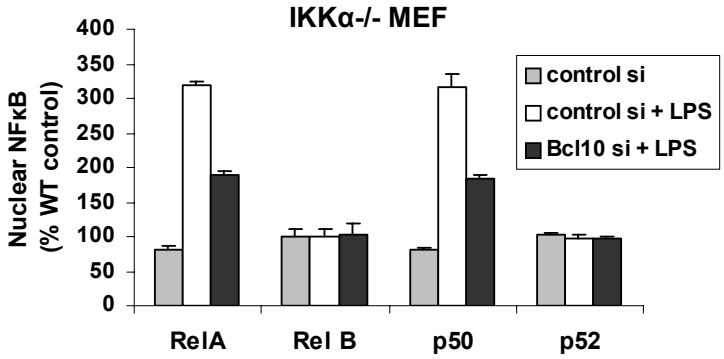

D

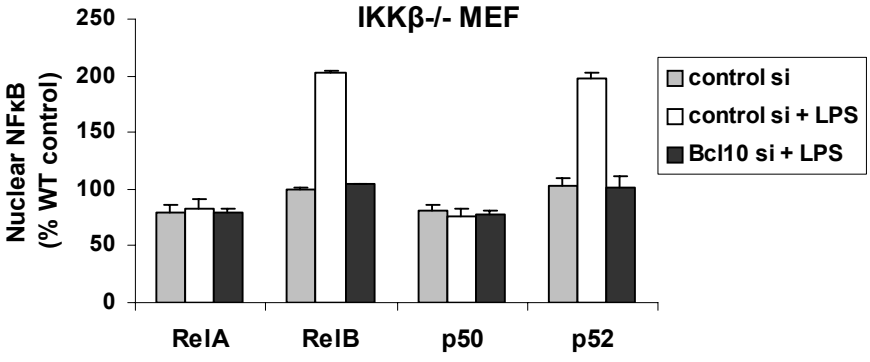

Figure 2.

A

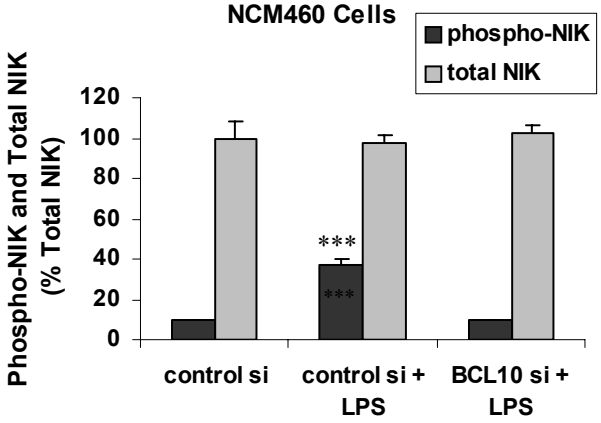

B

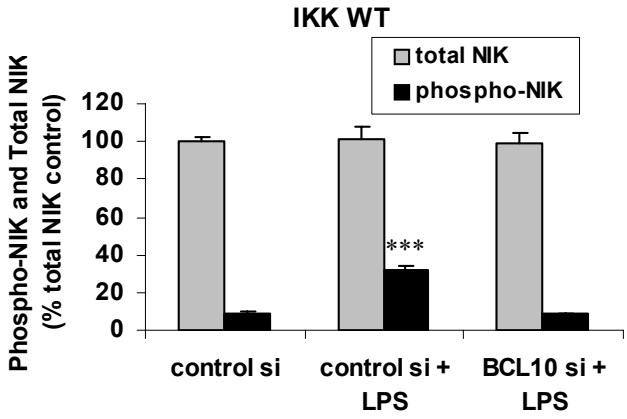

C

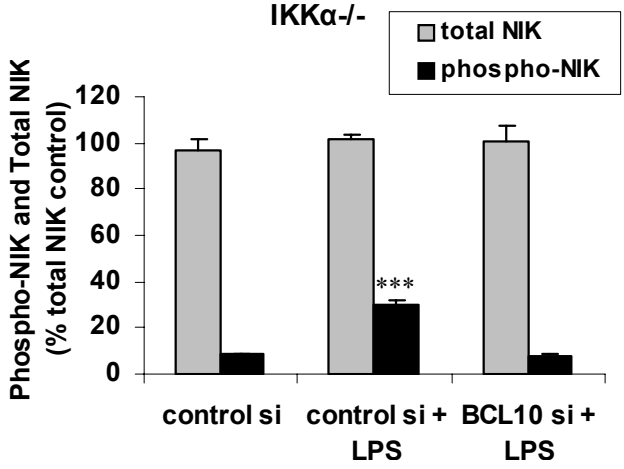

D

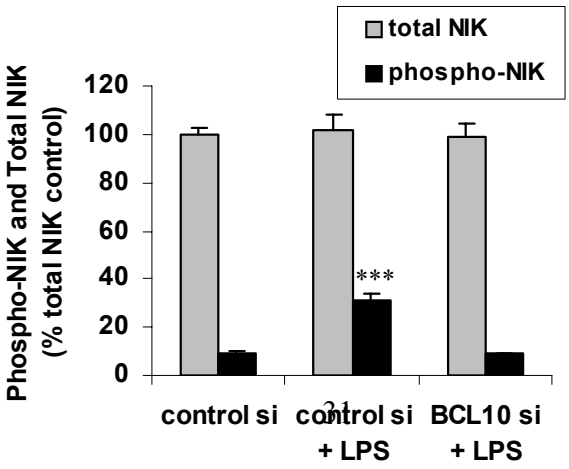

Figure 3. Total NIK

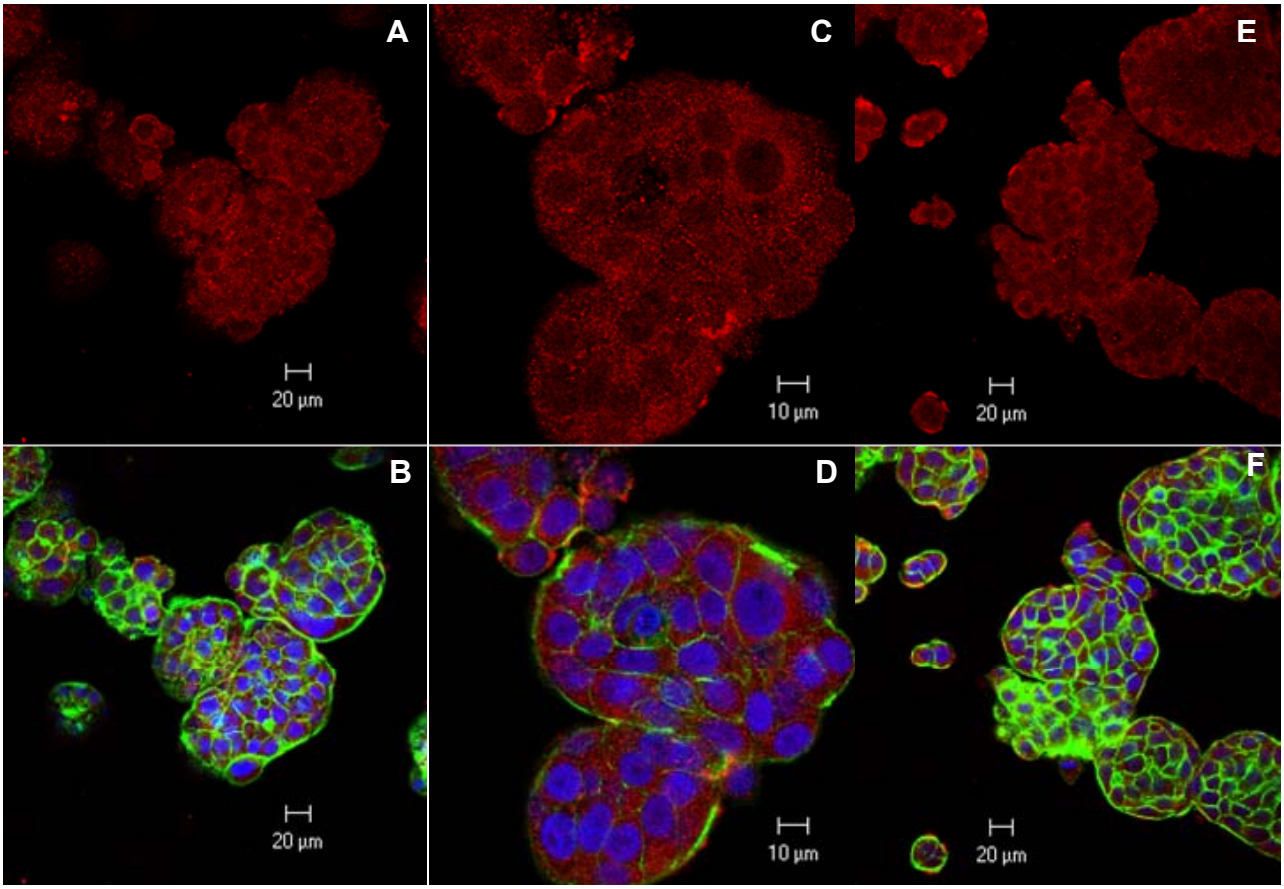

Control **LPS + control siRNA** **LPS + BCL10 siRNA**

Figure 4. Phospho-NIK

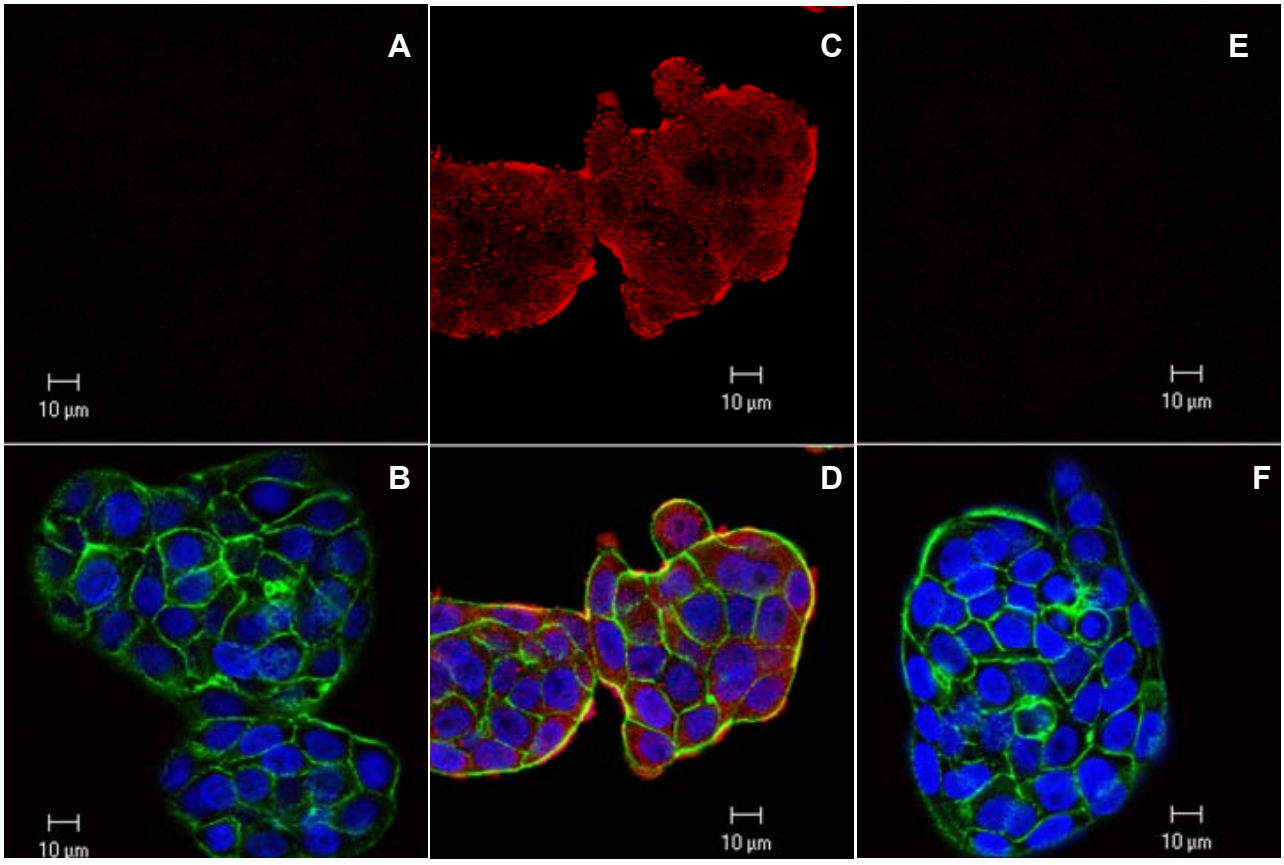

Control **LPS + control siRNA** **LPS + BCL10 siRNA**

Figure 5.

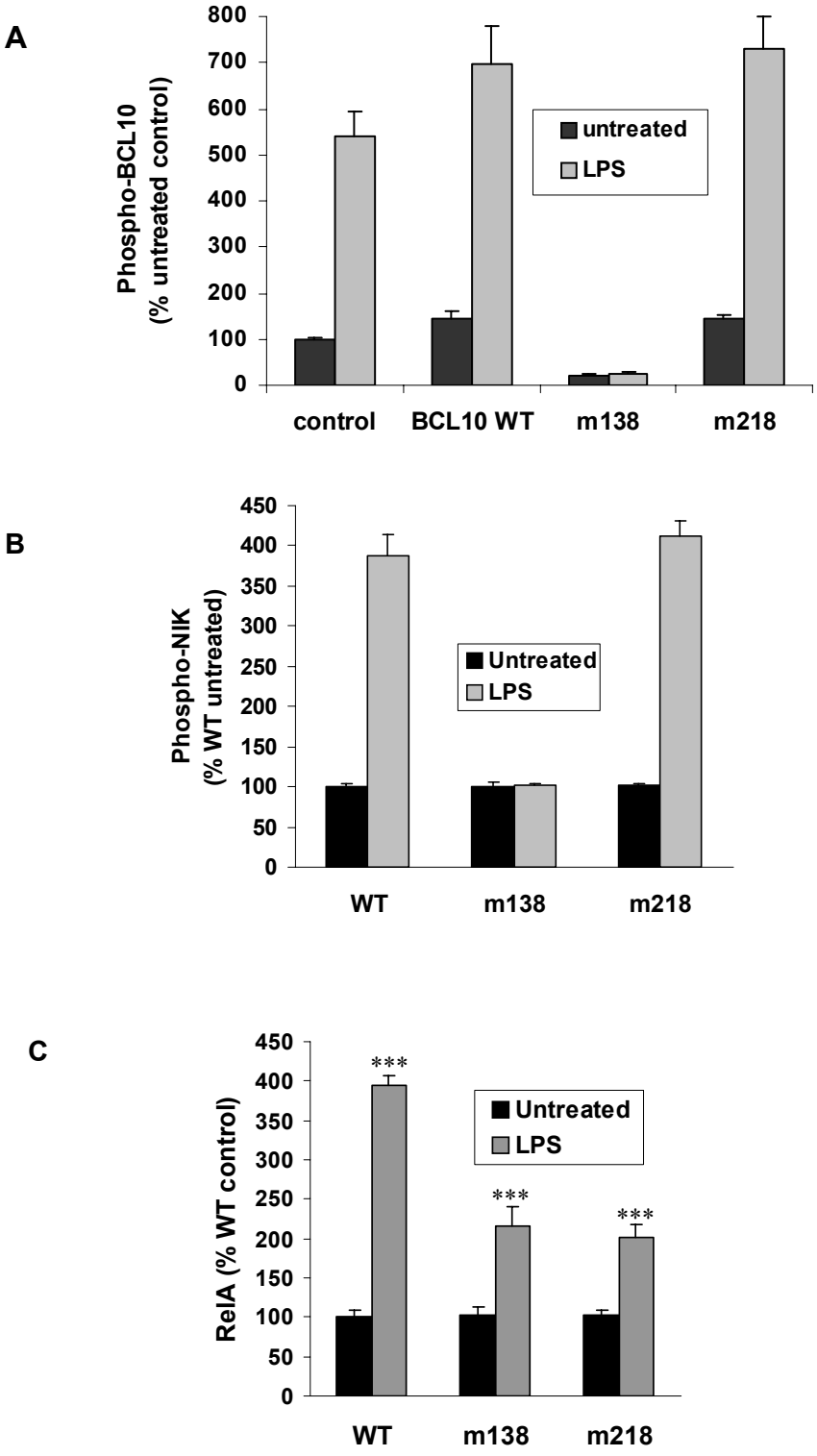
A
Phospho-BCL10
(% untreated control)
800
700
600
500
400
300
200
100
0
untreated
LPS
control
BCL10 WT
m138
m218
B
Phospho-NIK
(% WT untreated)
450
400
350
300
250
200
150
100
50
0
Untreated
LPS
WT
m138
m218
C
RelA (% WT control)
450
400
350
300
250
200
150
100
50
0
***
***
***
Untreated
LPS
WT
m138
m218

D

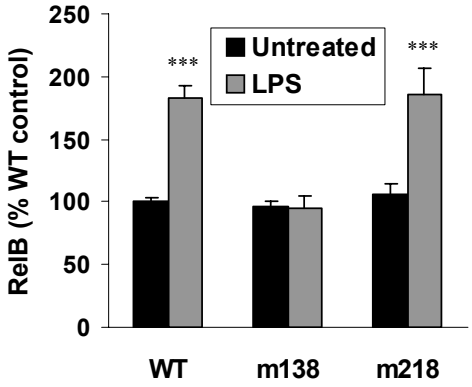
250
200
150
100
50
0
RelB (% WT control)
Untreated
LPS
***
***
WT
m138
m218

Figure 6.

A

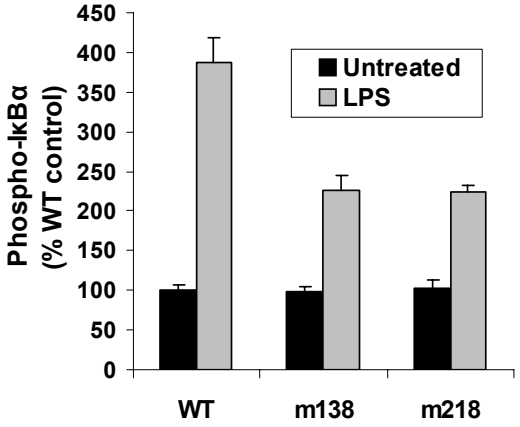
Phospho-IκBα (% WT control)
450
400
350
300
250
200
150
100
50
0
Untreated
LPS
WT
m138
m218

B

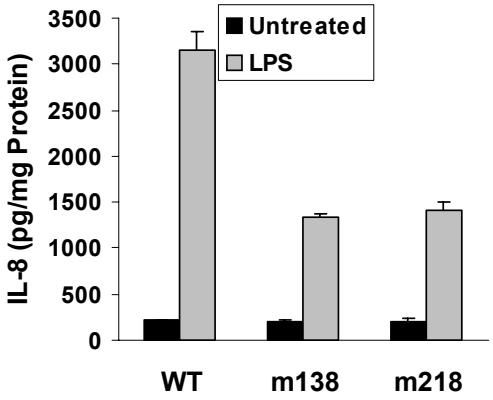
IL-8 (pg/mg Protein)
3500
3000
2500
2000
1500
1000
500
0
Untreated
LPS
WT
m138
m218

C

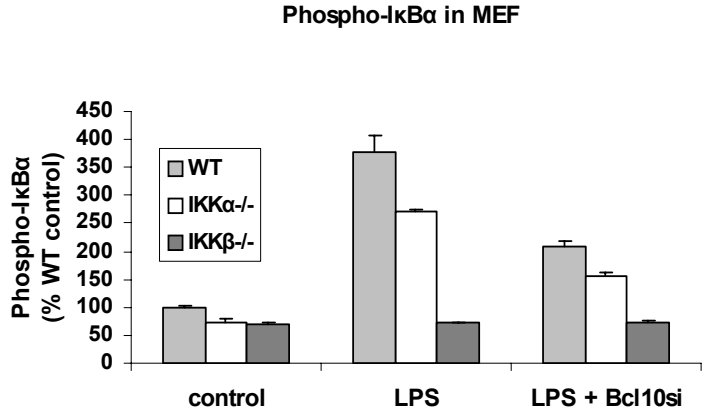
Phospho-IκBα in MEF
Phospho-IκBα (% WT control)
450
400
350
300
250
200
150
100
50
0
WT
IKKα-/-
IKKβ-/-
control
LPS
LPS + Bcl10si

D

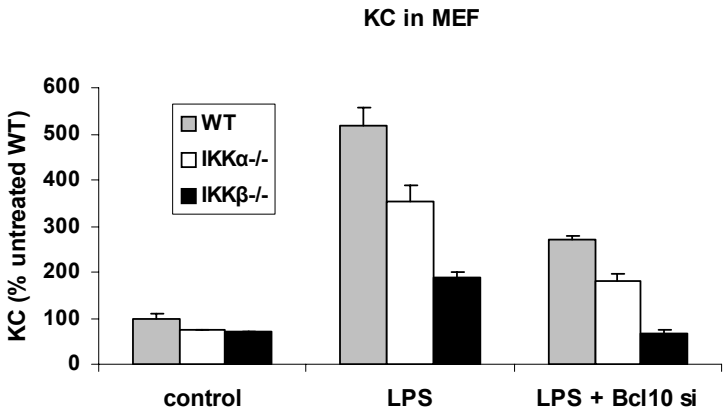
KC in MEF
KC (% untreated WT)
600
500
400
300
200
100
0
WT
IKKα-/-
IKKβ-/-
control
LPS
LPS + Bcl10 si

Figure 7.

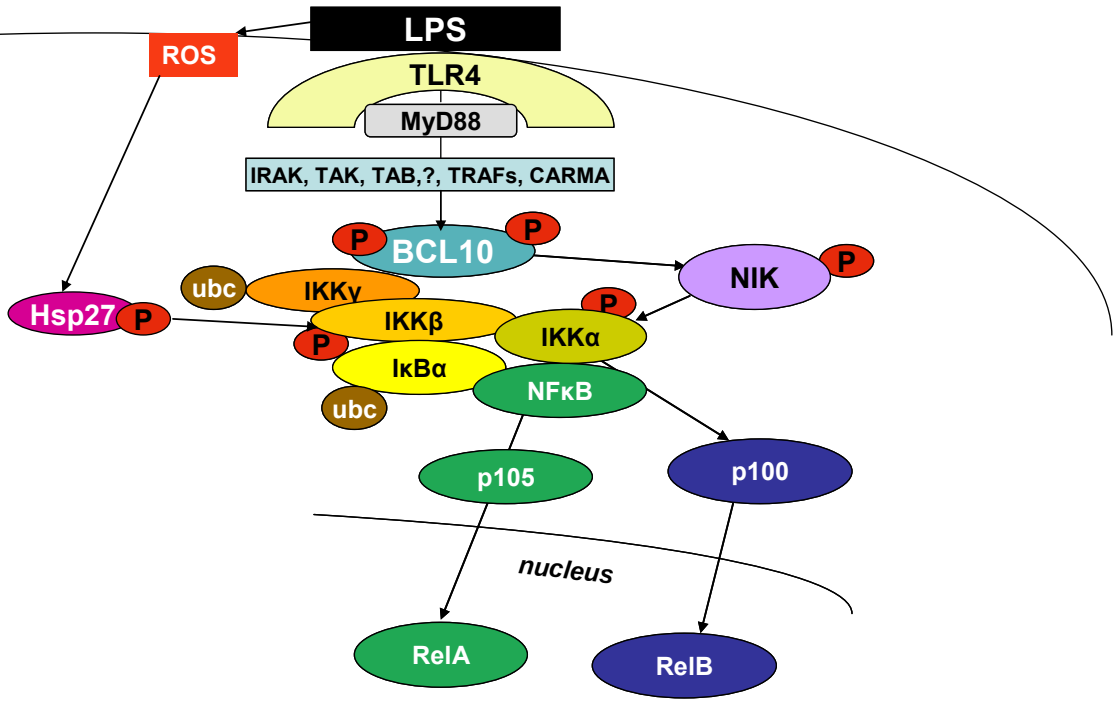
LPS
ROS
TLR4
MyD88
IRAK, TAK, TAB,?, TRAFs, CARMA
P
BCL10
P
NIK
P
ubc
IKKγ
Hsp27
P
IKKβ
P
P
IKKα
IκBα
NFκB
ubc
p105
p100
nucleus
RelA
RelB